Chapter 3
Numerical Modeling and Experimental Validation of Residual Stress Fields in Aluminum Alloy Induced by Shot Peening

H. Bae, C. Goodloe, A. Hossain, and M. Michaelis

Abstract Shot peening is a widely used cold working process that enhances the mechanical properties of metals by inducing compressive residual stresses through high-velocity particle impacts. These compressive stresses prevent the propagation of surface micro-cracks and are widely used in the aviation industry to replace grinding-induced tensile stresses. As a result, shot peening improves fatigue strength and stress corrosion resistance in metallic parts. Despite its long-standing industrial use, numerical modeling of shot peening remains challenging, especially in accurately capturing the complex interactions of multiple impacts. Most existing research focuses on single-shot peening, which is useful for sensitivity analysis but not for practical applications. This is because the real-world shot peening process involves multiple impacts, resulting in a cumulative residual stress field that cannot be accurately extrapolated from single-shot models. This study employs microscale finite element modeling to investigate the response of aluminum alloy 7050-T7451 under both single and multiple impacts during shot peening. A single-shot impact model is first developed using LS-DYNA to simulate indentation depths at various shot velocities. These simulated indentations are then compared to experimentally measured surface roughness data to identify the shot velocity that best matches the experimental results. This calibrated velocity is then used as an input for the multiple-shot impact model. The multiple-shot model, also developed in LS-DYNA, simulates a sequence of impacts using the selected velocity to estimate the resulting compressive residual stress field in the material. Finally, the simulated stress distributions are compared with experimental residual stress measurements to assess the model's accuracy and its ability to replicate real-world shot peening effects. These results contribute to a more accurate numerical approach for predicting residual stress in shot-peened components, offering insights into optimizing process parameters and enhancing fatigue performance in aerospace-grade aluminum alloys.

Keywords Shot Peening · FEA · Residual Stress · Fatigue · Aluminum Alloy

Introduction

Shot peening is one of the surface treatment methods to improve the strength, durability, and fatigue resistance of metal. It is a cold working process that uses a stream of small particles to produce compressive residual stress. The layer of plastic deformation induced by this process increases the resistance to stress corrosion cracking of metallic components. Hence, this method is widely used in many engineering applications to improve fatigue life and to achieve other mechanical properties.

Much research has been conducted, experimentally and/or numerically, to investigate the overall effects of shot peening on fatigue strength and other mechanical properties. For example, Farrahi et al. [1] conducted experimental studies to describe different shot peening parameters such as shot hardness, shot size and shot projection pressure on the residual stress distribution and fatigue life of spring steel. Based on their research work, a correlation was found between the fatigue strength and the area underneath the residual stress distribution curve. The largest shot size offered the best fatigue life improvement. However, the smaller shot size offered the best fatigue performance for a shorter time of shot peening. Hassani et al. [2] conducted a numerical study on shot peening using the finite element software ABAQUS. This research reported the displacement and stress distributions of the peened surface for three different scenarios, such as 1) single shot impacts normal to the target with three different impact velocities 2) multiple shot impacts (5-shots) normal to the target surface

H. Bae · C. Goodloe · A. Hossain · M. Michaelis
1075 Washington St. Cheney, WA 99004
e-mail: hbae1@ewu.edu; cgoodloe@ewu.edu; nhossain@ewu.edu; michaelis@ewu.edu

© The Author(s), under exclusive license to River Publishers 2026

Kaitlynn Fitzgerald et al. (eds.), *Fracture, Fatigue, Failure and Thermomechanics & Infrared Imaging, Volume 4, 2026*,
Conference Proceedings of the Society for Experimental Mechanics Series, https://doi.org/10.13052/rp-9788743816270

and 3) a single shot impact at an oblique angle to the peened surface. The peened surface was simulated using the standard 3D 8-node brick elements, where the shot was simulated as a rigid surface. The simulation considered the non-linear strain hardening and strain-rate dependency material properties. Their model discussed the importance of strain-rate in the context of displacement and stress distributions. Schiffner and Helling [3] used finite element software ADINA to simulate the shot peening process to predict the development, magnitude, and distribution of the residual stresses with different parameters, such as shot velocity, shot diameter and material parameters. In the first step, they used an axisymmetric model to simulate the perpendicular impact of an elastic sphere against an elastic–plastic peened surface. In a second step, it was shown how the results of the axisymmetric approach can be transformed into a three-dimensional model to investigate the effect of adjacent shots. Baragetti et al. [4–6] conducted several investigations to predict the residual stress developed by shot peening on steel surfaces. In one of the investigations, Design of Experiments (DoE) was applied to the results obtained by the numerical simulations where a smooth steel surface was impacted by one or more spheres. The research outcomes helped to choose the best peening parameters for different treatment conditions. In other works, the authors used finite element analysis, both axisymmetric and three dimensional, to predict in-depth residual stress field created on a material surface by shot peening process with different treatment parameters. Authors used different approaches to determine the numerical method that allows researchers to achieve the best results with the less expansive use of hardware and software. Eltobgy et al. [7] used an elasto-plastic finite element (FE) model in ABAQUS to simulate the shot peening process. The 3D FE model considered the material damping, thermal elastic-plastic material behavior, a rigid or deformable body for the shot and the effects of multiple shot impacts. The workpiece used in that simulation modelled the AISI 4340 steel at HRC 52 $\pm$ 2. The effects of strain hardening, strain rate and temperature were considered in the non-linear material model. The Johnson-Cook material model was employed to describe the stress behavior of the target material. The analysis employed a Lagrangian formulation with no interference between the incoming and rebounding shots. In this simulation, a master-slave based contact was used with isotropic Coulomb friction. Results showed that the predicted residual stress profile agreed well with published experimental results provided the shot was modelled as a deformable body and material damping was considered. J. Xu and W. J. Koch [8] developed a numerical model in LS-DYNA to provide an evaluation of the edge effects in the shot peening process. The research work considered both single impact and multiple impacts for part geometries with different edge radii. With this work, they predicted the residual stress profile around the target material's edge. Based on this research, a part with a relatively larger edge radius offered a satisfactory residual stress profile, which could equal or exceed that expected for a part with a smaller edge radius. Meguid et al. [9] and [10] developed 3D finite element models in ANSYS to simulate the shot peening process. In this research, single and double elasto-plastic impacts were examined using rigid spherical shots on metallic targets. The effect of shot velocity, size, shape, and target characteristics was analyzed on the residual stress distribution. This research also considered the effects of separation distance between the twin-shots on the residual stress field. It was found that effects of shot peening parameters, such as shot velocity, size, shape and separation distance between the twin shots have more effect on residual stresses than the strain-hardening rate of the target. Majzoobi et al. [11] investigated multiple shot impacts and effect of shot velocity on the residual stress profile using LS-Dyna. In this research, the effects of shot velocity and peening coverage were investigated. The residual stress distribution was found to be highly dependent on impact velocity and multiplicity. The increase of shot velocity was found to improve the residual stress distribution up to a particular point. In a recent study, Qian et al. [12] investigated the effects of shot peening pressure and shot coverage on the fatigue life of 20CrMnTi test specimens. This study also considered the effects of shot peening and re-shot peening on the fatigue life of shot-peened materials after different load cycles. The results showed that a reasonable shot peening pressure and coverage rate can improve the fatigue life of the test specimen to some extent, while a shot peening pressure higher than 0.4 MPa reduced the fatigue life. Re-shot peening removes the residual compressive stress relaxation on the surface of the material caused by cyclic loading and improves the fatigue life of the material.

From the literature review, it is found that most studies have focused on the single shot impact model to investigate the residual stress effect on the target specimen. Only limited research has been conducted to study the effect of multiple shot impacts. In addition, the numerical analysis results are mostly compared with experimental compressive residual stress results using XRD (X-Ray Diffraction). However, the XRD method is not feasible in practice because it is difficult to prepare the sample in the field. The surface roughness can be a means to validate the finite element model for the shot peening process. The depth of the plastic deformation from the finite element model can be compared with the experimentally measured surface roughness (Rt). Hence, there is additional need to provide a valid finite element model to simulate the effects of shot peening process by single and multiple impacts.

This research work investigated the microscale modeling of shot peening effects of Al 7050-T7451 test specimens subjected to single and multiple shot impacts. Numerical simulations were conducted using the finite element software LS-DYNA. The single impact model investigated the depth of the plastic deformation of the test specimen at two different shot velocities: 20 m/s and 30 m/s. The results from the simulations were compared with the corresponding experimental surface roughness profiles, Rt. The multiple shot impact model investigated the effect of repeated impacts and the subsequent cov-

erage of shot peening. The numerical results of the 30 m/s and 20 m/s shot velocities were both close to the experimental value of Rt. With 30 m/s having slightly more plastic deformation and 20 m/s having slightly less. These two velocities were used to give an upper and lower bound of results for other simulations performed using multiple shot analysis.

Experimental Procedure

Aluminum alloy 7050-T7451 blocks (100 mm X 100 mm) were used for this study. Material properties used in the study are listed in Table 1. The shot peening condition was cast steel shot S230, 172 kPa air pressure, 304 mm SOD, 90° impingement angle, 40.1 g/s shot flow rate and 0.24 mmA (0.01 A) intensity. A MarSurf XR 20 surface profilometer was utilized to measure the depth of the indentation on the shot peened surface. The compressive residual stresses of the shot peened samples were measured using the hole-drilling method. A carbide mill #38 FG inverted cone and strain gage type CEA-13-062UL-120 were employed in the hole-drilling experiments.

Table 1 Material Properties.

Property	Al 7050-T7451	Shot
Yield Strength (MPa)	469	572
Young's Modulus (GPa)	71.7	204
Poisson's ratio	0.33	0.27
Density (Kg/m^3)	2823	7916

Geometric Modeling of Single Shot Impact

An elastic-plastic nonlinear quasi-static finite element analysis was performed using the commercial software package LS-DYNA. The aluminum specimen used in this study was modeled as a flat block. The geometry configuration was 1 mm in X and Z directions and 3 mm in Y direction, respectively. The appropriate mesh size was 0.05 mm. The steel shot was a spherical shape with 0.29 mm in radius and also was meshed. Figure 1 shows the geometry and finite element mesh of the model. The finite element mesh was generated using LS-PREPOST.

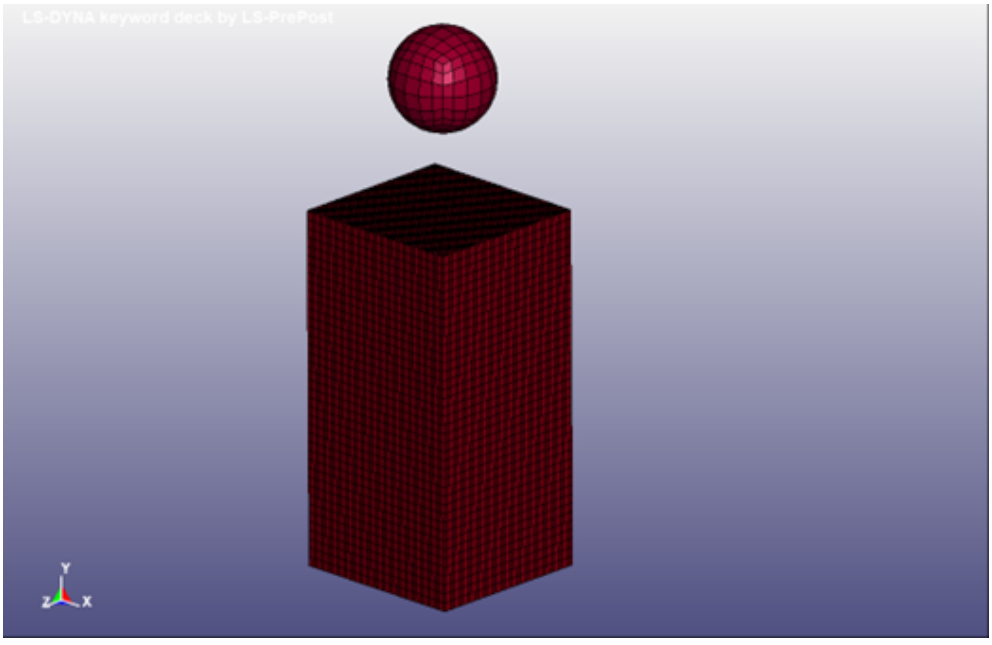

Fig. 1 Geometry and Finite Element Mesh for the Single Shot Analysis.

The contact algorism used "surface to surface" algorithm. The master-slave contact algorithm was used with the constraint that the specimen and the shot do not penetrate each other. Coulomb friction model with a coefficient of 0.2 was used in this model. After a shot impacts the surface of the specimen the shot rebounds. Each shot was only allowed to impact the surface once.

Strain hardening was included in this model to determine the plastic deformation. The material's stress–strain behavior was represented using a piecewise linear plasticity formulation. By adjusting the model parameters, this approach can simulate the full range of metallic behavior, from linear elastic to elastic–perfectly plastic response. The relationship between effective plastic strain and the corresponding yield stress is presented in Figure 2. The shot material was hard steel with the compressive yield stress 572 MPa, Poisson's ratio $\nu = 0.27$, Young's modulus E = 204 GPa, and density $\rho = 7916$ kg/m^3.

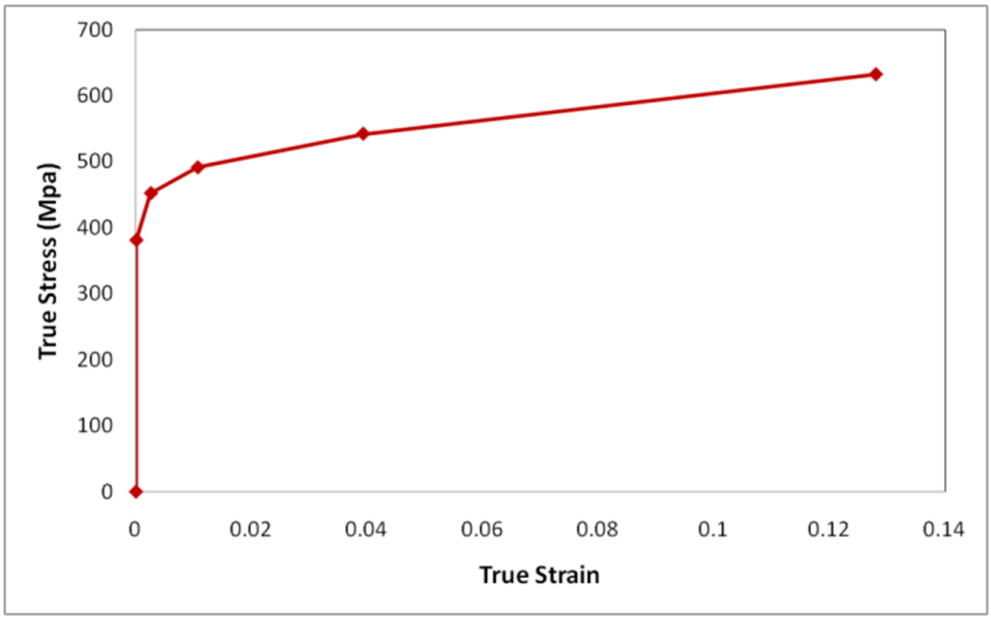

Fig. 2 Experimental Stress-Strain Curve of Al 7050-T7451.

Single Shot Impact Analysis Result

The effect of shot velocity on the plastic deformation was investigated. Since the shot velocity could not be measured experimentally, four simulation shot velocities, 20 m/s, 30 m/s, 40 m/s and 50 m/s, were chosen arbitrarily and all shots traveled along the Y-direction. In Figure 3, the depth of the plastic deformation was compared with measured surface roughness, R_t.

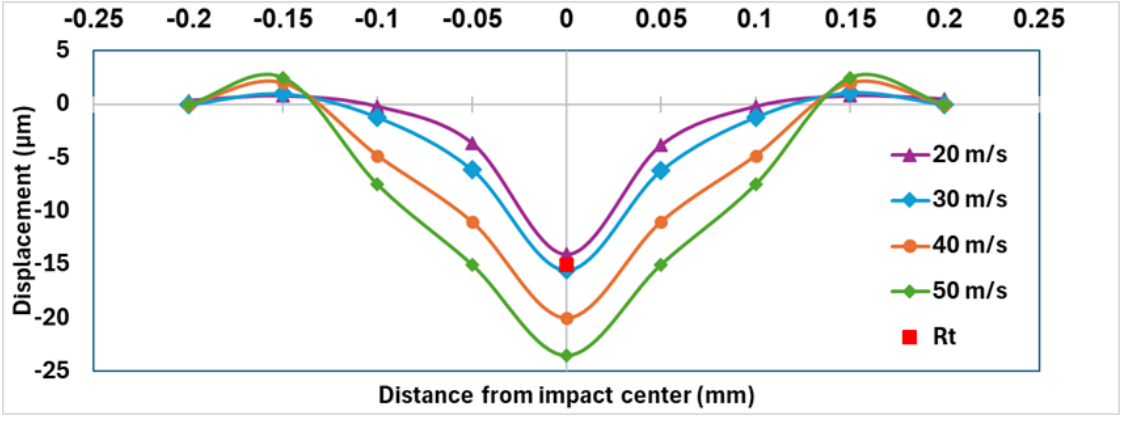

Fig. 3 Displacement Results from Two Different Shot Velocity Analysis.

It is shown that higher velocity induces an increase in the depth of the plastic deformation. It appears that the highest plastic deformations are 14 μm at the velocity of 20 m/s, 15 μm at the velocity of 30 m/s, 20 μm at the velocity of 40 m/s, and 23 μm at the velocity of 50 m/s. The maximum plastic deformation was 23 μm. The experimental data point R_t falls closely between the maximum depth points for 20 m/s and 30 m/s.

Geometric Modeling of Multiple Shot Impact

Eight multi-shot impact models were developed to evaluate the residual stress fields at varying coverage levels and shot velocities. Specifically, eight finite element models were employed for the multi-shot analysis, consisting of two 4-shot models, two 8-shot models, two 13-shot models, and two 16-shot models. The finite element models for multiple impacts were constructed similarly to the single shot impact model. The finite element meshes for both the workpiece and the shots were identical to those used in the single shot analysis. Both the 20 m/s and 30 m/s models were chosen for the multi shot analysis. Both results have close matches with the surface roughness value (R_t).

The 4-shot, 8-shot, 13-shot and 16-shot impact models were built to examine the effect of the 28% 52%, 72%, and 100% coverages. Figure 4 shows the microscopic images of shot peened surfaces at four different coverage levels. All models were built to investigate the shot peening coverage effect. They were designed to minimize repeated impacts at the same location. From the single shot analysis, it is found that the dimple size from the shot impact is 0.3 mm. To minimize the overlapping of the indentations, 0.3 mm dimple size was chosen as the shot's distance. Figure 5 shows the arrangement of the shots used in the multiple shot impact models. The blue circles indicate the shot indentations. The blue circles are placed to minimize to overlap each other. The 4-shot, 8-shot, 13-shot and 16-shot impact models were built to examine the effect of the 28% 52%, 72%, and 100% coverages. Figures 6, 7, 8, and 9 show the geometries of the shot impact models for each coverage.

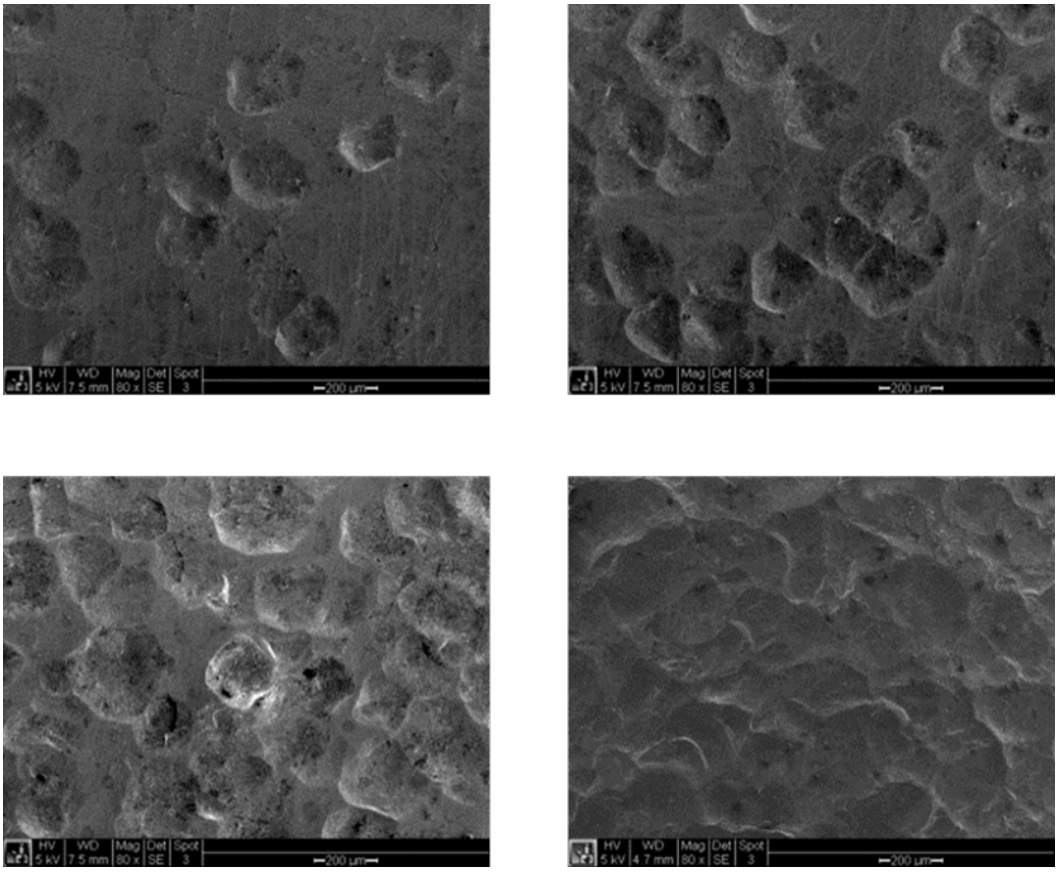

Fig. 4 Microscopic Images of Shot-peened Samples at Four Different Coverage Levels (Top Left: 28%, Top Right: 52%, Bottom Left: 72% And Bottom Right: 100%).

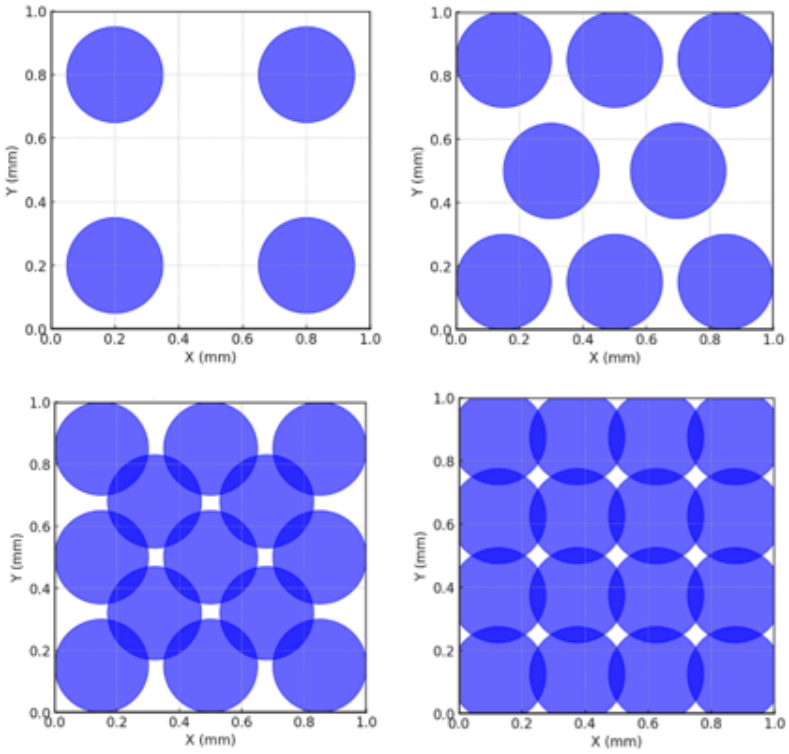

Fig. 5 Shot Arrangements used in the Multiple Shot Impact Models (Top Left: 28%, Top Right: 52%, Bottom Left: 72% And Bottom Right: 100%).

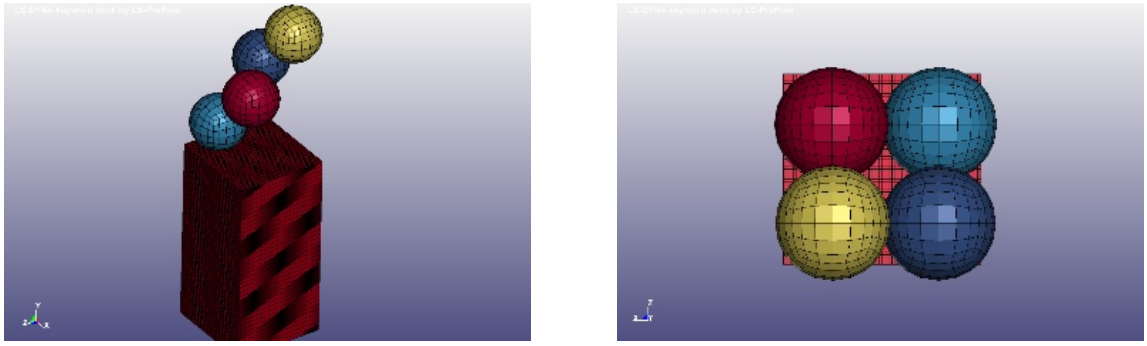

Fig. 6 Geometry and Finite Element Mesh for the 4-Shot Analysis (28% Coverage).

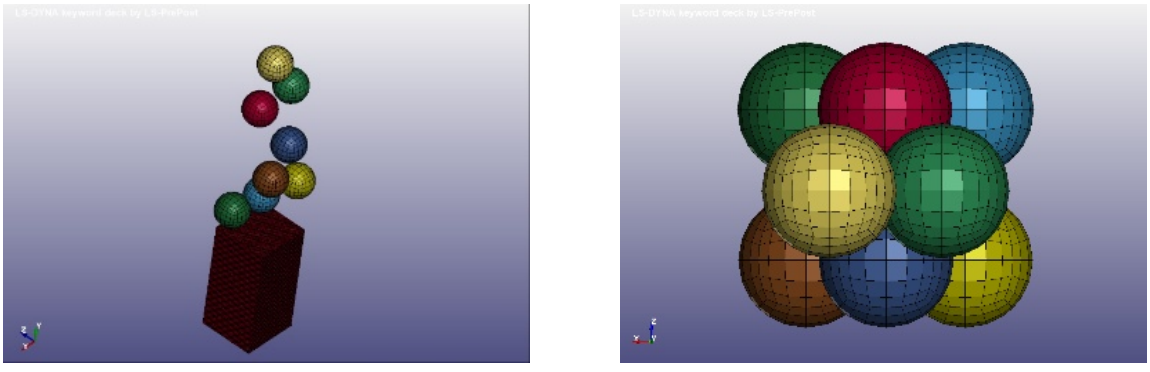

Fig. 7 Geometry and Finite Element Mesh for the 8-Shot Analysis (52% Coverage).

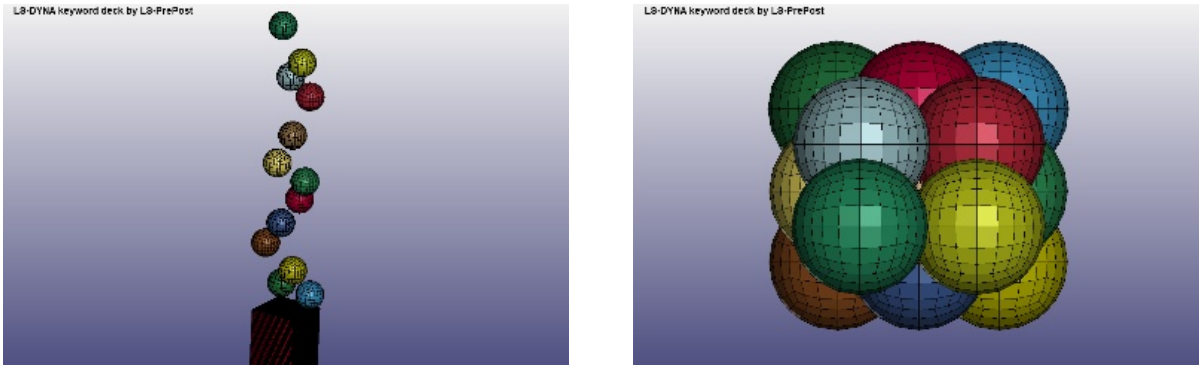

Fig. 8 Geometry and Finite Element Mesh for the 13-Shot Analysis (72% Coverage).

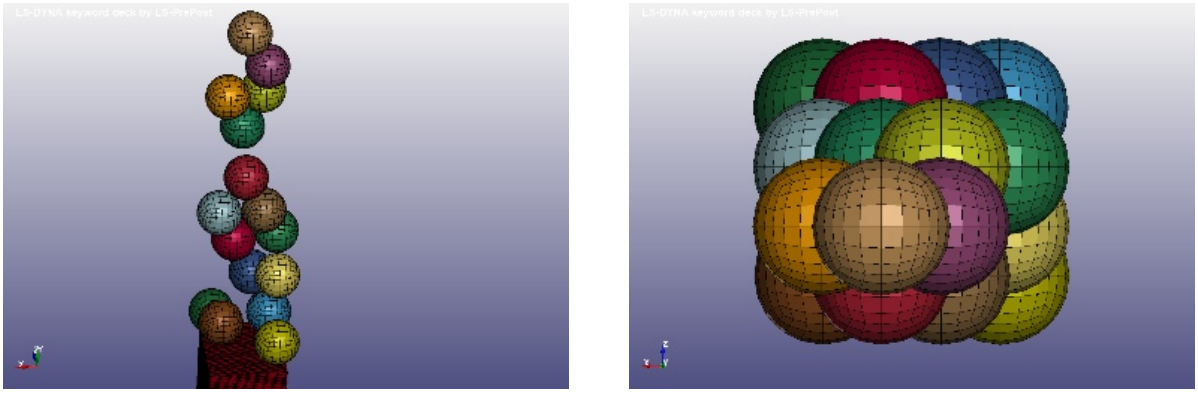

Fig. 9 Geometry and Finite Element Mesh for the 16-Shot Analysis (100% Coverage).

Results And Discussion

The Von Mises stress distribution along the surface of the 20 m/s and 30 m/s models are shown in Figures 10 and 11. In each figure, the top-left image corresponds to 28% coverage, the bottom-left to 52% coverage, the top-right to 72% coverage, and

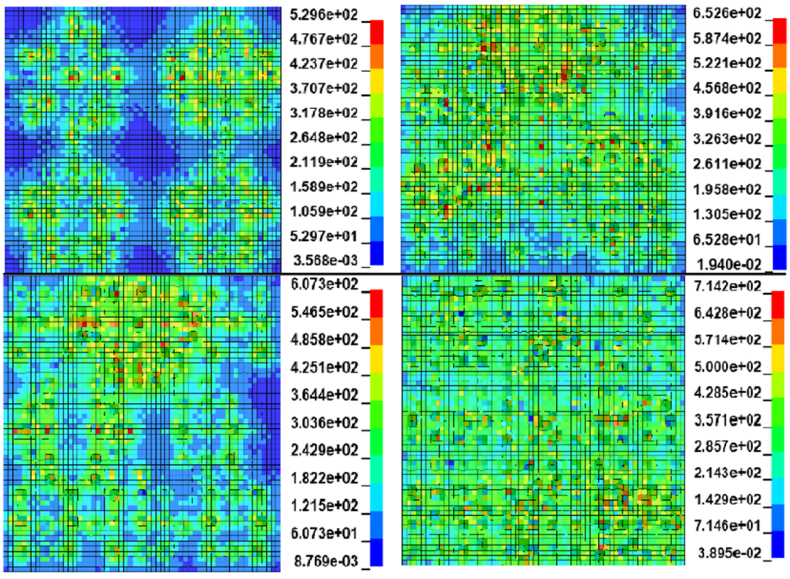

Fig. 10 Von Mises Stress Distribution in MPa for 20 m/s Multi Shot Models (Top Left: 28%, Bottom Left: 52%, Top Right: 72% And Bottom Right: 100%).

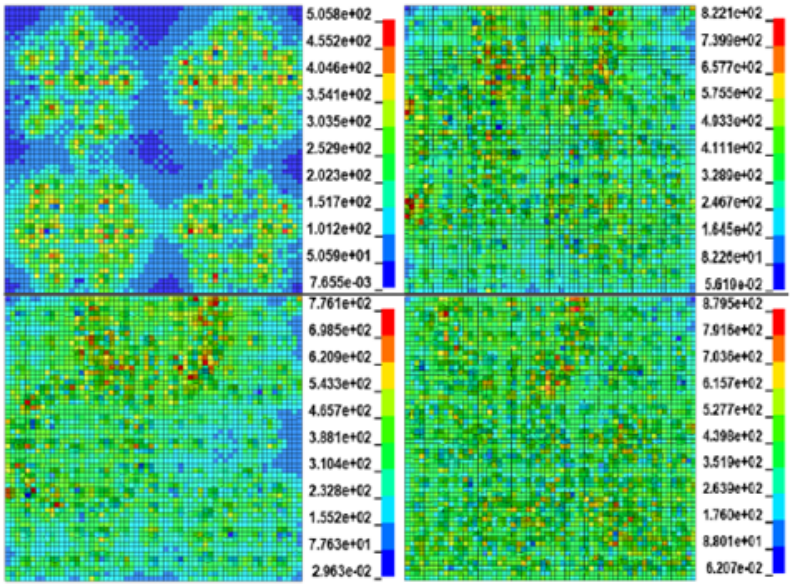

Fig. 11 Von Mises Stress Distribution in MPa for 30 m/s Multi Shot Models (Top Left: 28%, Bottom Left: 52%, Top Right: 72% And Bottom Right: 100%).

the bottom-right to 100% coverage. A color-coded stress scale is shown to the right of each image. Stress values are reported in MPa, where red indicates the highest stress in the model and blue indicates the lowest. The 30 m/s models exhibit higher stress intensity and fewer regions of low stress compared to the 20 m/s models. At lower coverage levels (28% and 52%), the higher velocity models also show a broader stress distribution.

The multi-shot simulations evaluated how impact distribution influences the stress fields formed in and around the dimples. For each coverage model (Figure 12), surface compressive stress was extracted as von Mises stress along predefined

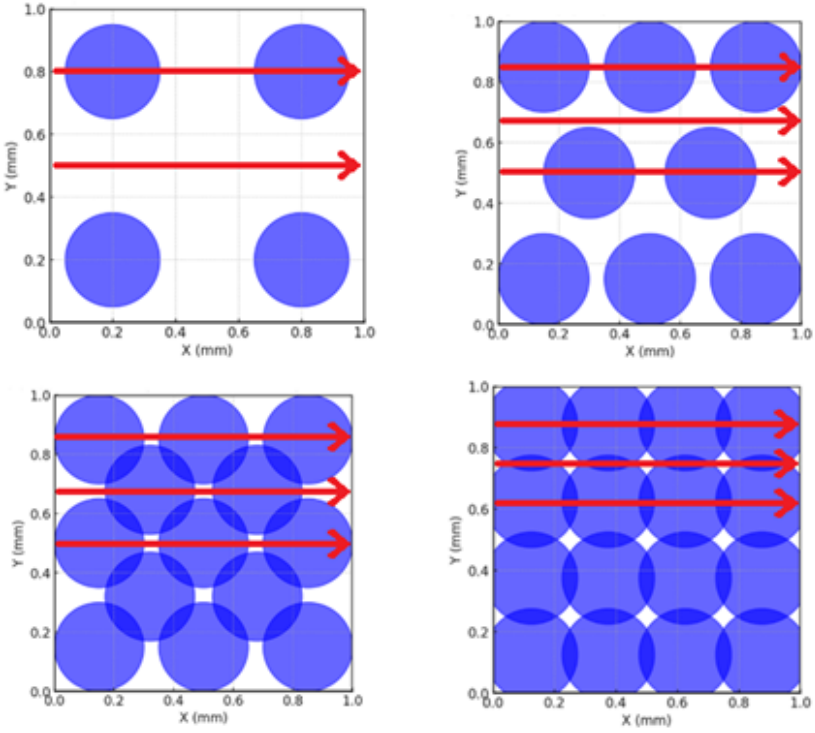

Fig. 12 Data Collection Patterns for Each Coverage.

rows representing unique impact patterns, and the values were averaged and compared with experimental hole-drilling results. In the four-shot case, two lines were selected through the impact centers and between impacts. The eight-shot case used three lines through three impact centers, two impact centers, and the intermediate region. The thirteen-shot case also used three lines through edge impacts, central impacts with significant overlap, and the intermediate impacts. Similarly, the sixteen-shot case included lines through edge impacts, closely spaced central impacts with strong stress-field interaction, and the region between them without direct impacts.

Numerical Results

For each coverage level, the residual stress fields were compared with experimental values obtained from hole-drilling measurements. Figures 13–16 present the compressive stress distributions along the surface of the four coverage models at 20 m/s and 30 m/s, compared with the experimental results. The circles represent the average stress values, while the capped lines indicate the data range after outlier removal.

For the 28% (four-shot) coverage shown in Figure 13, minimal difference was observed between the 20 m/s (268 MPa) and 30 m/s (266 MPa) models, though both averages were significantly higher than the experimental value (145 MPa). The

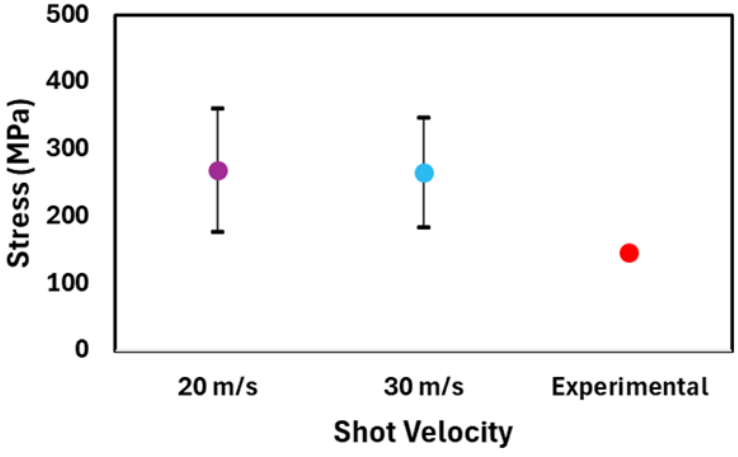

Fig. 13 Average Stresses for 28% Coverage Sample at 20 m/s and 30 m/s with Experimental Value.

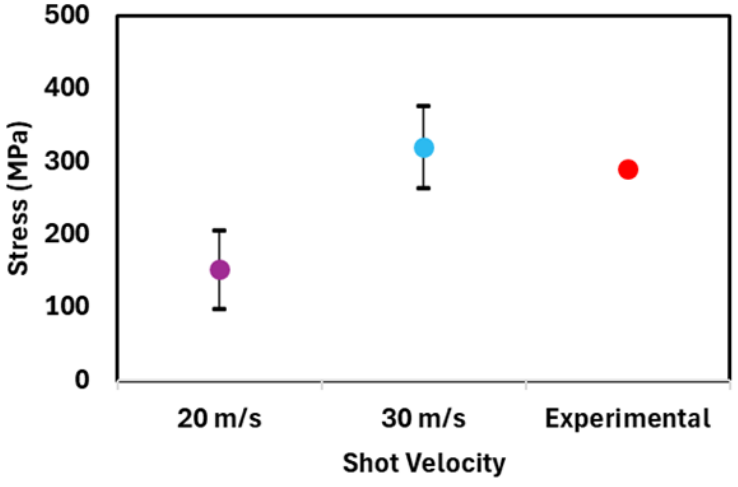

Fig. 14 Average Stresses for 52% Coverage Sample at 20 m/s and 30 m/s with Experimental Value.

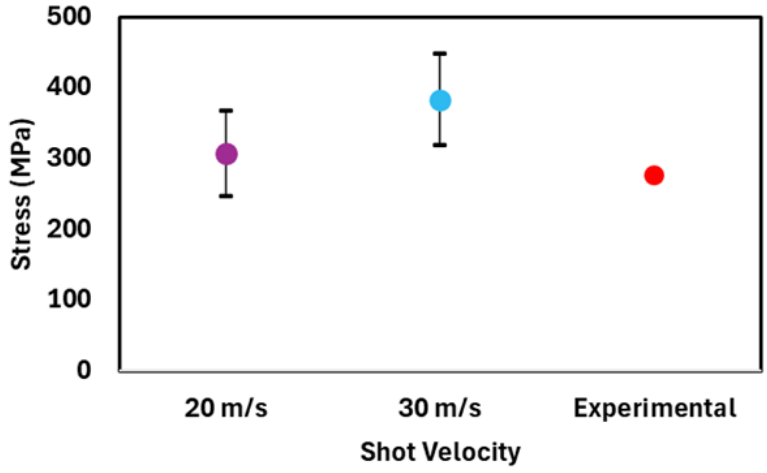

Fig. 15 Average Stresses for 72% Coverage Sample at 20 m/s and 30 m/s with Experimental Value.

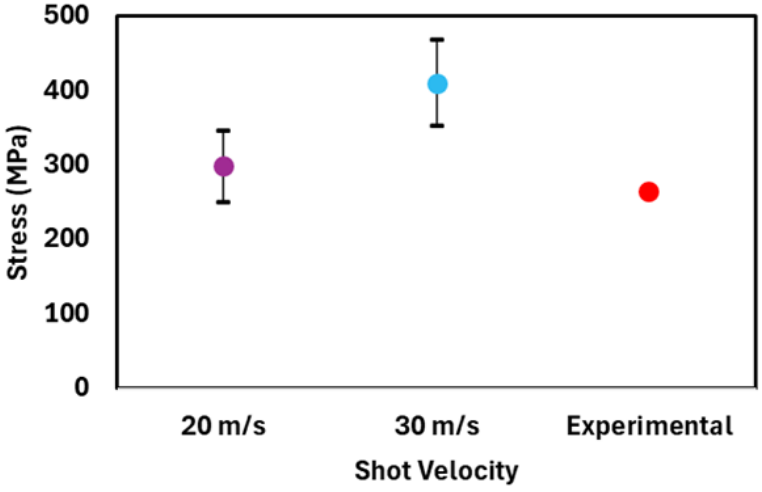

Fig. 16 Average Stresses for 100% Coverage Sample at 20 m/s and 30 m/s with Experimental Value.

stress ranges were broad, indicating substantial variability. Although the experimental value fell within both ranges, neither model accurately reproduced the experimental average.

In Figure 14, the 52% coverage model exhibited a narrower stress distribution. The experimental value (289 MPa) fell within the range of the 30 m/s model but not within that of the 20 m/s model.

For the 72% coverage (Figure 15), the experimental value (277 MPa) fell within the range of the 20 m/s model. Increased coverage resulted in significant impact overlap, which elevated stress levels in overlapping regions. At this coverage, the 20 m/s model more closely matched the experimental average.

At 100% coverage (Figure 16), the narrowest stress distributions were observed due to the absence of zero-stress regions. The experimental value was 265 MPa, and under this condition, the 20 m/s model most closely matched the experimental result.

Overall, at each coverage level, at least one numerical model contained the experimental value within its stress range. Stress variability decreased with increasing coverage, and agreement with experimental data improved. The 30 m/s model provided better agreement at lower coverages, whereas the 20 m/s model showed closer agreement at higher coverages.

The relatively uniform compressive residual stress distribution produced by the 100% coverage model is illustrated in Figure 17. Localized stress peaks are observed beneath individual impact sites, where the compressive stresses penetrate deeper into the substrate. In contrast, the surface layer exhibits a more uniform and consistently elevated compressive stress

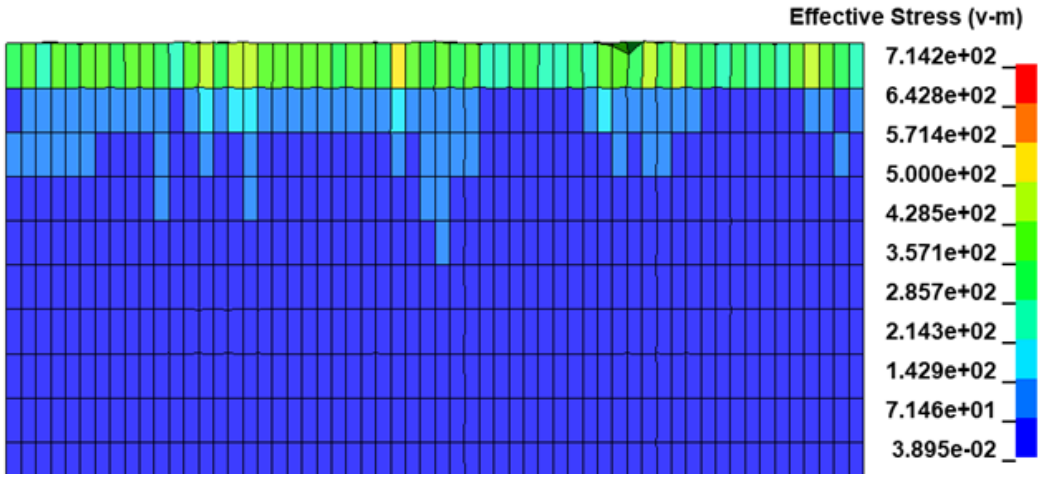

Fig. 17 Von Mises Stress Distribution for the 100% Coverage Model at 20 m/s, Shown on a Sectional Cut Through the Center of the Model.

state. This distribution confirms the ability of shot peening to generate a stable compressive surface layer, which is critical for enhancing fatigue resistance by mitigating crack initiation and early crack propagation.

The stress distribution with depth is critical to the effectiveness of the treatment. Figure 18 presents the compressive residual stress as a function of depth along a sectional cut through the center of the model. The data were extracted from one of the central element columns. The results show an increase in compressive stress immediately beneath the surface, followed by a gradual decrease with increasing depth. Importantly, the surface maintains a non-zero compressive stress, which contributes to improved fatigue life. Additionally, the stress coverage remains consistent across the surface, as previously shown in Figure 17, with no zero-stress regions even at locations distant from the impact centers.

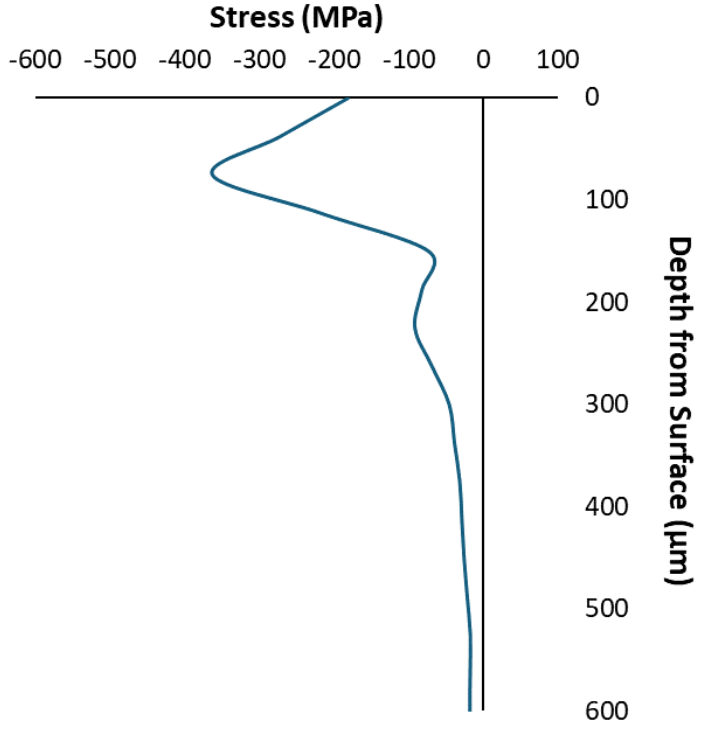

Fig. 18 Compressive Residual Stress Distribution with Depth for the 100% Coverage Model at 20 m/s.

Conclusion

This study extended previous single-shot peening modeling to validate multi-shot simulations against experimental results. The objective was to investigate how increasing surface coverage influences the distribution of compressive residual stress and to compare those numerical results with experimental stresses obtained from hole-drilling measurements.

The results for varying coverage levels (28%, 52%, 72%, and 100%) demonstrated that increasing coverage improved agreement between the numerical models and experimental data. At higher coverages, both the stress range and average values approached the experimental results. The 20 m/s model at 100% coverage provided the closest agreement, with an average compressive stress compared to the experimental value.

The surface stress distribution for the 20 m/s, 100% coverage model was consistently elevated, with no regions of low or zero stress observed. This uniform compressive layer further supports the capability of the model to replicate the behavior of actual shot peening processes.

Overall, the results indicate that as coverage increases, the 20 m/s model more accurately reproduces experimental residual stress measurements, whereas at lower coverages the 30 m/s model provides closer agreement. These findings are consistent with previous work [13], where the 30 m/s single-shot model best matched experimental surface roughness. However, as the number of impacts increases, the higher-velocity models tend to overpredict surface stress, reducing agreement with experimental residual stress values.

Acknowledgments The authors acknowledge support from Eastern Washington University and the facilities provided for experimental and computational work.

References

1. G. H. Farrahi, J. L. Lebrun and D. Couratin, “Effects of Shot Peening on Residual Stress and Fatigue Life of a Spring Steel”, *Fatigue and Fracture of Engineering Materials and Structure*, Vol. 18, No. 2., pp. 211-220, 1995.
2. S. T. S. Al-Hassani, “Numerical Simulation of Multiple Shot Impact”, 7th *International Conf. on Shot Peening*, 1999.
3. K. Schffner and C. Droste gen. Helling, “Simulation of Residual Stresses by Shot Peening”, *Computers and Structures 72*, pp.329-340, 1999.
4. S. Baragetti, “Non-dimensional analysis of shot peening by means of DoE”, *International Journal of Materials and Product Technology*, Vol. 15, No. 1-2, 2000.
5. S. Baragetti, M. Guagliano and S. Vergani, “A Numerical Procedure for Shot Peening Optimization by Means of Non-dimensional Factors”, *International Journal of Materials and Product Technology*, Vol. 15, No. 1-2, 2000.
6. S. Baragetti, “Three-Dimensional Finite-Element Procedures for Shot Peening Residual Stress Field Prediction”, International Journal of Computer Applications in Technology, Vol. 14, No. 1-3, 2001.
7. M. S. ElTobgy, E. Ng and M. A. Elbestawi, “Three-dimensional Elastoplastic Finite Element Model for Residual Stresses in the Shot Peening Process”, *Proc.Instn Mech. Engrs*, Vol. 218, pp.1471-1481, 2004.
8. J. Xu and W. J. Koch, “Finite Element Analysis of the Influence of Workpiece Edge Geometry on Shot Peening Process”, J. Aerosp. Eng. Vol. 22, pp.153, 2009.
9. S. A. Meguid, G. Shagal, J. C. Stranart and J. Daly, “Three-dimensional Dynamic Finite Element Analysis of Shot-Peening Induced Residual Stresses”, *Finite Elements in Analysis and Design 31*, pp.179-191, 1999.
10. S. A. Meguid, G. Shagal and J. C. Stranart, “3D FE Analysis of Peening of Strain-rate Sensitive Materials Using Multiple Impingement Model”, *International Journal of Impact Engineering 27*, pp.119-134, 2002.
11. G. H. Majzoobi, R. Azizi, A. Alavi Nia, “A Three-Dimensional Shot Peening Process using Multiple Shot Impacts”, Journal of Materials Processing Technology, 164-165, pp. 1226-1234, 2005.
12. W. Qian, Y. Wang, K. Liu, X. Yin, X. He, and L. Xie, “Experimental Study on the Effect of Shot Peening and Re-Shot Peening on the Residual Stress Distribution and Fatigue Life of 20CrMnTi”, Coatings, Vol. 13., No. 1210, 2023.
13. H. Bae, M. Ramulu, A. Hossain, ”Microscale Modeling to Study Shot Peening Effects on Aluminum Alloy.”, ASME International Mechanical Engineering Congress and Exposition, vol. 50640, p. V010T13A010. American Society of Mechanical Engineers, 2016.